

# Metadata of the chapter that will be visualized in SpringerLink

Book Title	Biogenic—Abiogenic Interactions in Natural and Anthropogenic Systems 2022	
Series Title		
Chapter Title	Surface Properties of Carbonate Speleothems in Karst Caves Changing Under Biofilms	
Copyright Year	2023	
Copyright HolderName	The Author(s), under exclusive license to Springer Nature Switzerland AG	
Corresponding Author	Family Name	<b>Sofinskaya</b>
	Particle	
	Given Name	<b>Oxana A.</b>
	Prefix	
	Suffix	
	Role	
	Division	
	Organization	Kazan (Volga Region) Federal University
	Address	Kazan, Russia
	Email	ushik2001@mail.ru
Author	Family Name	<b>Andrushkevich</b>
	Particle	
	Given Name	<b>Oleg Y.</b>
	Prefix	
	Suffix	
	Role	
	Division	
	Organization	Kazan (Volga Region) Federal University
	Address	Kazan, Russia
	Email	
Author	Family Name	<b>Galiullin</b>
	Particle	
	Given Name	<b>Bulat M.</b>
	Prefix	
	Suffix	
	Role	
	Division	
	Organization	Kazan (Volga Region) Federal University
	Address	Kazan, Russia
	Email	
Author	Family Name	<b>Gogoleva</b>
	Particle	
	Given Name	<b>Nataliya E.</b>
	Prefix	
	Suffix	

Role  
Division  
Organization Kazan (Volga Region) Federal University  
Address Kazan, Russia  
Email

---

Author Family Name **Shaikhutdinov**  
Particle  
Given Name **Nurislam M.**  
Prefix  
Suffix  
Role  
Division  
Organization Kazan (Volga Region) Federal University  
Address Kazan, Russia  
Email

---

Author Family Name **Korolev**  
Particle  
Given Name **Eduard A.**  
Prefix  
Suffix  
Role  
Division  
Organization Kazan (Volga Region) Federal University  
Address Kazan, Russia  
Email

---

Author Family Name **Mouraviev**  
Particle  
Given Name **Fedor A.**  
Prefix  
Suffix  
Role  
Division  
Organization Kazan (Volga Region) Federal University  
Address Kazan, Russia  
Email

---

Author Family Name **Usmanov**  
Particle  
Given Name **Rustem M.**  
Prefix  
Suffix  
Role  
Division  
Organization Kazan (Volga Region) Federal University  
Address Kazan, Russia  
Email

---

## Abstract

Some surface properties of carbonate speleothems from Kirillov's, Pionerskaya and Yaschik Pandory caves in the Republic of Khakasia, as well as Yuryevskaya Cave in the Republic of Tatarstan were investigated. The types of the speleothem samples such as crusts, drips, corallites, and moon milk were studied. All the samples were collected in cave aphotic zones at a wall temperature not higher than + 10 °C. Differently polished marble onyx, gypsum and glass plates were taken as reference surfaces. The surfaces were processed by polishing, heating, etching chemicals, and adding R2A modified growth media. These modes simulated experimentally common natural processes in the system of "calcium carbonate –chemolithotrophic biofilm". The speleothem samples under the cave microbial community, which can exist successfully in the upper soil layer, were considered against the background of the reference mineral surfaces. The captive bubble method, SEM, XRD, EDX, as well as DTG analyses were carried out to determine wettability, roughness, total organic matter content, and elemental and mineral compositions of the samples. The metagenome of the microbial community was estimated using 16S rRNA sequence analysis. The influence of fresh and long-lived biofilms on the carbonate surface properties is assessed. The assumption that biofilm dynamics affects the carbonate surface properties and its toughness is substantiated. Our work hypothesized that the part of organic matter can enter the gaps in growing carbonate crystals, then, is sealed with a new mineral phase, and later, is assimilated by heterotrophic and organotrophic organisms.

---

Keywords  
(separated by '-')

Wettability - Organic matter - Surface roughness - Biocement toughness - Biofilm dynamics -  
Extremophiles - Chemolithotrophs - Biomorphs - Pseudomorphoses

---

# Surface Properties of Carbonate Speleothems in Karst Caves Changing Under Biofilms



**Oxana A. Sofinskaya, Oleg Y. Andrushkevich, Bulat M. Galiullin, Nataliya E. Gogoleva, Nurislam M. Shaikhutdinov, Eduard A. Korolev, Fedor A. Mouraviev, and Rustem M. Usmanov**

**Abstract** Some surface properties of carbonate speleothems from Kirillov's, Pioneer-skaya and Yaschik Pandory caves in the Republic of Khakasia, as well as Yuryevskaya Cave in the Republic of Tatarstan were investigated. The types of the speleothem samples such as crusts, drips, corallites, and moon milk were studied. All the samples were collected in cave aphotic zones at a wall temperature not higher than + 10 °C. Differently polished marble onyx, gypsum and glass plates were taken as reference surfaces. The surfaces were processed by polishing, heating, etching chemicals, and adding R2A modified growth media. These modes simulated experimentally common natural processes in the system of "calcium carbonate—chemolithotrophic biofilm". The speleothem samples under the cave microbial community, which can exist successfully in the upper soil layer, were considered against the background of the reference mineral surfaces. The captive bubble method, SEM, XRD, EDX, as well as DTG analyses were carried out to determine wettability, roughness, total organic matter content, and elemental and mineral compositions of the samples. The metagenome of the microbial community was estimated using 16S rRNA sequence analysis. The influence of fresh and long-lived biofilms on the carbonate surface properties is assessed. The assumption that biofilm dynamics affects the carbonate surface properties and its toughness is substantiated. Our work hypothesized that the part of organic matter can enter the gaps in growing carbonate crystals, then, is sealed with a new mineral phase, and later, is assimilated by heterotrophic and organotrophic organisms.

**Keywords** Wettability · Organic matter · Surface roughness · Biocement toughness · Biofilm dynamics · Extremophiles · Chemolithotrophs · Biomorphs · Pseudomorphoses

---

O. A. Sofinskaya (✉) · O. Y. Andrushkevich · B. M. Galiullin · N. E. Gogoleva · N. M. Shaikhutdinov · E. A. Korolev · F. A. Mouraviev · R. M. Usmanov  
Kazan (Volga Region) Federal University, Kazan, Russia  
e-mail: [ushik2001@mail.ru](mailto:ushik2001@mail.ru)

© The Author(s), under exclusive license to Springer Nature Switzerland AG 2023  
O. V. Frank-Kamenetskaya et al. (eds.), *Biogenic—Abiogenic Interactions in Natural and Anthropogenic Systems 2022*, Springer Proceedings in Earth and Environmental Sciences, [https://doi.org/10.1007/978-3-031-40470-2\\_29](https://doi.org/10.1007/978-3-031-40470-2_29)

1

## 1 Introduction

Carbonate formations are promising objects for the design of biocement structures and protective (transport) capsules for microflora, as well as for the refinement of the geologic record (Melim et al. 2016). The surface properties of carbonate formations are closely related to biofilms developing on them (Mouraviev et al. 2006; Banks et al. 2010; Tugarova 2021). Biofilms have a life cycle, at each stage of which they can affect the covered surface differently either destroying or preserving it (Andryukov et al. 2020; Zorina et al. 2019). The interaction between autochthonous or inoculated biofilms and the carbonate leads to the deposition or destruction of minerals and isomorphic replacement in crystal lattices, which should be taken into account when using cements and other carbonate-based materials in geotechnologies (Gray and Engel 2013; Banks et al. 2010; Glazovskaya and Dobrovolskaya 1984; Guvensen et al. 2013; Pronk et al. 2017; Wischart et al. 2019; Leonova et al. 2015). Hereby, both lithoautotrophic and organoheterotrophic modes of microbial metabolism can destroy carbonates. In the first case, this occurs due to biogenic acids production, and in the second case, due to carbon dioxide release (Gray and Engel 2013). Carbonate precipitation requires microbial communities to shift the pH of their environment toward the alkaline side, for example, via alkalis releasing or sulfate reduction (Leonova et al. 2015). Calcium carbonate precipitation passes four stages—amorphous, vaterite, aragonite, and calcite, among which calcite is the only thermodynamically stable phase, while others are metastable. However, the presence of organic matter in the environment is proved to be an inhibitor on the metastable phase transformation and thus, makes them possible to coexist (Myszka et al. 2019).

In our work, we have simulated experimentally some of the mechanical and chemical effects that can be induced by chemolithotrophic biofilms on the carbonate. From the extended version of the DLVO theory, fineness, roughness, hydration, and the type of contact between particles are known to be the factors significant for particle adhesion strength (Andryukov et al. 2020). Carbonate biofilm can affect each of them. Both the abilities to disperse and to stick particles together are peculiar to microbial communities (Gray and Engel 2013; Banks et al. 2010; Glazovskaya and Dobrovolskaya 1984; Pronk et al. 2017). Particles disintegrate via the dissolution of the cement binding them in aggregates. Particle aggregation begins either by a gel forming in the extracellular polymer substances (EPS) or by a cement precipitating in gaps between particles. Surface roughness is similarly formed by biofilms, however, herewith the latter affect only the aggregates' surfaces but not intra-aggregate bonds. The hydration of biofilm-coated particles most strongly depends on the stage of biofilm development: a fresh biofilm can attach to a particle only if the latter has hydrophobic contact. It produces the hydrophobic substances that promote the strongest attachment to the surface (Zorina et al. 2019; Andryukov et al. 2020). Nevertheless, for sufficient nutrition delivered as an aqueous phase, the biofilm is forced to produce hydrophilic compounds. Thus, fluctuations in the hydrophilic-hydrophobic properties of the substrate surface occur. This leads to the alternation of strengthening and weakening contacts between particles. In the presence of a

68 hydrophilic surface, particles form coagulates; and vice versa, in the presence of  
 69 a hydrophobic one, particles can reversibly aggregate, as well as form direct point  
 70 contacts, after which the cementation or crystallization contacts are likely.

71 Based on the dynamic behavior of biofilms concerning the coated mineral phase  
 72 and considered the previous studies (Melim et al. 2016) it can be hypothesized that a  
 73 part of the organic matter enters the gaps between growing crystals through selective  
 74 adsorption and/or capillary condensation. Then, these substances can be sealed with a  
 75 new mineral phase, and thus preserved. Further, under the acids episodically released  
 76 by the biofilm and etching a mineral phase, the organic matter is reactivated and can  
 77 be consumed by heterotrophic and organotrophic organisms. The purpose of this  
 78 work was to check this hypothesis.

## 79 2 Sites and Sampling

80 Carbonate speleothem samples were purposefully selected from totally different  
 81 geologic zones (Fig. 1). Karst genesis, the contact of clayey deposits with carbonate  
 82 rocks, 3–sevenfold excess of the atmospheric partial pressure of CO<sub>2</sub>, aphotic zones,  
 83 and the wall temperatures not higher than + 10 °C were the common features of the  
 84 sampling sites. The samples were taken from the walls and cornices of caves in such  
 85 a way as to exclude anthropogenic and zoogenic pollution as much as possible.

86 *Yurjevskaya Cave* (Fig. 1a) is a horizontal corridor system in Permian sedimentary  
 87 gypsum-dolomite rocks with a total length of about 1,5 km. It is located on the right

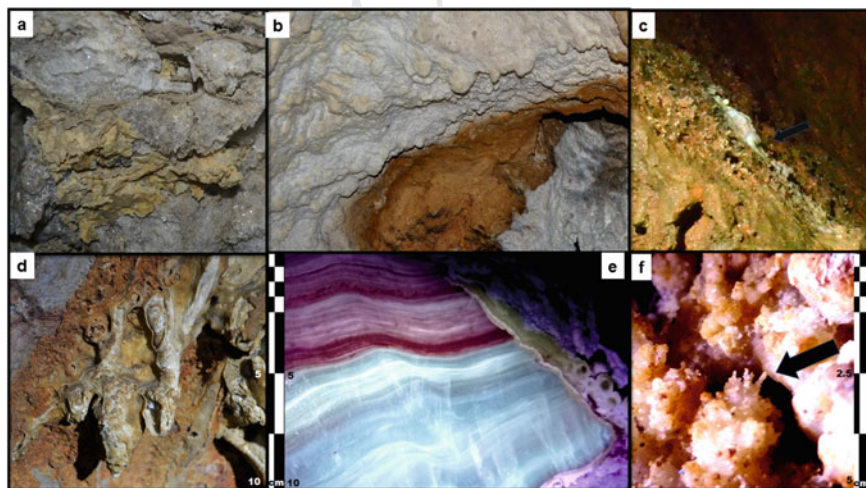


**Fig. 1** Some speleothems sampled from caves: **a** Yurjevskaya, crusts; **b** Pionerskaya, dry moon milk; **c** Pionerskaya, fresh moon milk; **d** Yaschik Pandory, drape; **e** Pionerskaya, marble onyx; **f** Yaschik Pandory, corallite with helictites

88 bank of the Volga River in the Republic of Tatarstan. Crust-type speleothems were  
89 selected from the Hall of Organ Pipes located 190 m far from the entrance. This  
90 hall is less attended by tourists compared to the neighboring ones. There was a wall  
91 temperature of + 4,0 °C, a air temperature of + 13,0 °C, and a relative air humidity  
92 of 67%.

93 *Pionerskaya Cave* (Fig. 1b, c, e) is a slightly inclined horizontal gallery with a  
94 maximum depth of 15 m and a total length of 86 m in Riphean dolomites (Nomokonov  
95 1969) with calcite mines located on the left bank of the Bely Iyus River (the Ob River  
96 basin) in the Republic of Khakasia. Sampling points were selected at a distance of  
97 20, 33 and 40 m far from the entrance, which ensured complete coverage of the cave  
98 along its length. The speleothem samples were «moon milk» at the different stages  
99 of drying, spherulites, and stalactites. There was an average wall temperature of +  
100 0.7 °C. The air temperature was from + 5,2 °C to + 8,0 °C rising from the entrance  
101 to the end. A relative air humidity was from 76 to 85%.

102 *Kirillov's Cave* is an inclined horizontal gallery with a maximum depth of 36 m  
103 and a total length of 320 m in massive Cambrian limestones (Nomokonov 1969)  
104 located inside a hill that is 400 m above the right bank of the Bely Iyus River.  
105 Somewhere there is an ice floor. Sampling points were selected at a distance of 13,  
106 39 and 68 m far from the entrance of the lower gallery and covered the cave wing,  
107 which is the richest in speleothems. The samples collected were small stalactites. A  
108 wall temperature increased from -6,0 °C to -0.8 °C from the entrance to the end as  
109 the gallery rose; an average air temperature was + 5,9 °C, and a relative air humidity  
110 was from 75 to 77%.

111 *Yaschik Pandory Cave* (Fig. 1d, f) is a system of vertical and inclined wells with  
112 a total depth of 180 m and a total length of about 11 km in the Cambrian rocks,  
113 which are represented by argillaceous limestones, sandstones, siltstones, gravelites  
114 up to a depth of 40 m, and there appear marls, diabases, porphyrites in the deeper  
115 layers (Nomokonov 1969). In some areas there the carbonate rock transition into  
116 marble occurs, probably due to the contact metamorphism in the zone of geologic  
117 faults. The cave is situated on the left bank of the Bely Iyus River, and is connected  
118 hydraulically with it on the lowermost floor. The samples were collected from depths  
119 of 0, 100, and 180 m below the entrance. There were spherulites, small stalactites,  
120 and corallites. The wall and air temperatures decreased from + 7 °C to + 4 °C and  
121 from + 18 °C to + 4 °C, respectively, and a relative air humidity increased from 68  
122 to 90% as descending to the bottom.

123 **Experimental impact on the samples.** Freshly sampled speleothems were placed  
124 into strong aluminum foils at an initial humidity, a temperature of + 12(±2) °C,  
125 and total darkness to preserve the active autochthonous biofilm. These samples  
126 participated in our experiment in the following modes: untreated slices, variously  
127 polished plates, ones powdered to sizes < 250 microns, heat-treated powders at 105  
128 and 525 °C, as well as chemically treated powders.

129 The mechanical treatment of a few samples was carried out in order to examine the  
130 effect of roughness and surface layer removal on the properties of natural carbonate  
131 formations. Marble onyx plates were processed in the following ways:

- 132 – *zero polishing*–untreated slices;  
133 – *polishing No. 1*–with a grinding disc grit of 75 microns and the creation of surface  
134 roughness at a level of 20–25 microns with oriented hatching;  
135 – *polishing No. 2*–with a grinding disk grit of 20 microns and the creation of surface  
136 roughness at a level of 8–12 microns with oriented hatching;  
137 – *polishing No. 3*–with free abrasive SiC M 14 and a uniformly rough surface at a  
138 level of 5–8 microns;  
139 – *polishing No. 4*–with free abrasive SiC M 10 and a uniformly rough surface at a  
140 level of 2–4 microns.

141 The samples were heated in order to dehydrate the surface (at 105 °C) and  
142 accelerate the removal of chemically bound water and organic matter (at 525 °C).

143 The chemical treatment of the samples was aimed at the release of the hypothetical  
144 organic matter from mineral chambers in two ways: by mineral etching and by the  
145 extraction of the organic matter with a solvent. The minerals were etched using oxalic,  
146 citric, acetic, hydrochloric, and sulfuric acids, commonly secreted by lithotrophic  
147 microorganisms (Glazovskaya and Dobrovolskaya 1984). The organic matter was  
148 extracted from the samples into NaOH and ethanol solutions (Golovanova 2022).

149 The fresh chemolithotrophic biofilm was stimulated by the modified R2-based  
150 growth medium intended for psychrophilic oligotrophs (Wischart et al. 2019;  
151 D’Angeli et al. 2017). The difference from the base R2 medium layed in the addi-  
152 tion of an alkaline humus extract and a triple compared to the base medium CaCO<sub>3</sub>  
153 content. The increased content of CaCO<sub>3</sub> was applied to establish the ionic equilib-  
154 rium between the studied surfaces and the washing solution, as well as to selectively  
155 stimulate the organisms adapted to carbonate metabolism. The humus extract was  
156 applied as a pH buffer for its natural level of 7.68–8.02, as well as a model for the  
157 contact of carbonate formations with the upper soil layer. Thus, the stimulation was  
158 aimed at those members of the cave community that can successfully exist in surface  
159 soil conditions.

### 160 3 Methods

161 The main surface investigation methods included contact angle measurement, SEM,  
162 EDX, TG-DSC, and XRD analyses. The contact angle is an indicator of both  
163 hydrophilic-hydrophobic properties and surface roughness. It was determined using  
164 the captive bubble method in the author’s modification for clay fraction powder  
165 specimens (Sofinskaya et al. 2022). The powders were stuck onto flat glass using  
166 adhesive tape at a pressure of 30 kPa, after which they were placed into an atmo-  
167 sphere with a relative air humidity of >96% for several minutes to saturate the pores  
168 with capillary-condensed moisture. Next, the specimens were immersed into a ther-  
169 mostatic bath of an optical tensiometer with deionized water, and an air bubble was  
170 placed and photographed on the powder/water interface. The images obtained were  
171 adjusted using the ImageJ program and then contact angles were calculated by the



172 Contact Angle Option. The representation of the measurements consisted of 30–100  
173 per a specimen depending on its surface stability.

174 Most of the samples were examined with a FEI XL-30ESEM scanning electron  
175 microscope. The SEM was carried out at a low vacuum mode under an acceler-  
176 ating voltage of 20 keV. Elemental analysis was performed using an EDAX energy  
177 dispersive spectrometer operating in combination with the SEM, based on which the  
178 mineral composition was calculated from the ratio of the weight of elements on the  
179 surface.

180 X-ray diffraction analysis was carried out with a D2 Phaser diffractometer (Bruker,  
181 Germany) in order to detail the mineral composition. Analysis mode was an X-ray  
182 tube voltage of 30 kV, a current of 30 mA, and the scanning step of 0.02° at a speed of  
183 1 deg/min. The range of scanning angles in the Bragg–Brentano geometry was from  
184 3 to 40°. Standard powder preparations were used. The qualitative and quantitative  
185 mineral composition was determined using the DIFFRAC.EVA and TOPAS software.

186 Thermal analysis was carried out with an STA 449 JupiterF3 device to determine  
187 the boiling point of the structural components of the samples. The burning interval  
188 was from 30 to 1000 °C, the heating step was 10 deg/min. with continuous air purging.  
189 There the reference Al<sub>2</sub>O<sub>3</sub>, which did not give a thermal effect within the temperature  
190 range from 20 to 1200°, was applied.

191 Taxonomic profiling of the bacterial communities was performed using S-D-Bact-  
192 0341-b-S-17 and S-D-Bact-0785-a-A-21 primers (Klindworth et al. 2013) targeting  
193 V3 and V4 regions of the 16S rRNA gene. The libraries were sequenced in the “Reg-  
194 ulatory genomics” lab of Kazan Federal University (Kazan, Russia) on the MiSeq  
195 (Illumina, USA) platform using the 2 × 300 bp paired-end MiSeq Reagent Kit v3. To  
196 process the sequencing data, we used the dada2 microbiome data denoising pipeline  
197 (version 1.14.0). The dada2 pipeline is based on sequencing error correction algo-  
198 rithms and generates exact amplicon sequence variants (ASVs). The dada2 pipeline  
199 implements the Naive Bayes classifier method for taxonomy assignment (Callahan  
200 et al. 2016). This classifier compares sequence variants with a training set of classified  
201 sequences, the Silva (version 138) rRNA gene database (silva\_nr99\_v138.1\_train\_  
202 set.fa), which is currently considered the most comprehensive 16S rRNA database  
203 of all microorganisms. To visualize and filter the processed data, a package written  
204 in the R programming language - phyloseq (McMurdie and Holmes 2013) was used.  
205 Data filtering was carried out to remove artifacts generated during the analysis. A  
206 set of samples passed through a bioinformatics pipeline with the same parameters.

## 207 4 Results

208 **Wetting contact angle (CA).** Finely polished marble onyx (*polishing No. 2, 3, 4*) is  
209 a hydrophilic matter with a fairly small standard deviation (StDev) of CA fluctuating  
210 within the observed range of 28° to 38° (Table 1, see *polishing No. 3*). It is noteworthy  
211 that the finest *polishing No. 4* caused a StDev rising (i.e., surface heterogeneity) due

212 to an increase in the range of CA observed at both ends of their distribution, which  
 213 is probably followed the artifacts introduced after polishing at dimension hatching  
 214 less than 5  $\mu\text{m}$ .

215 The *polishing No. 2* and *No. 1* had a larger range of CA variation than finely  
 216 processed ones, i.e., here macro-roughness was set by irregularities larger than 8  $\mu\text{m}$ .  
 217 The coarse polishing led to the splitting of one mode of the quasi-Gaussian CA  
 218 distribution into two, resulting in a bimodal distribution. Herewith, the low-angle  
 219 mode remained close to surfaces after fine polishing, while the high-angle mode  
 220 exceeded the maximum CA observed on these surfaces. The *zero polishing* sample  
 221 also had two CA distribution modes, of which the low-angle one was close to the  
 222 high-angle mode for a roughly polished surface (*polishing No. 1*), and the high-angle  
 223 one belonged to the hydrophobic range. That is, hydrophobic properties were set by  
 224 heterogeneities with a size of more than 25  $\mu\text{m}$  corresponded to the order of biofilm  
 225 thickness (Wagner and Horn 2017)

226 The speleothem powders had practically the same CA distribution parameters as  
 227 the *zero polishing* sample. Nevertheless, after dehydration at 105 °C the hydrophobic  
 228 heterogeneities and bimodal CA distribution disappeared and the distribution param-  
 229 eters approached surfaces with *polishing No. 1, 2, 3*. Heat treatment at 525 °C led to  
 230 a strong increase in surface heterogeneity (according to an increase in StDev), but  
 231 unless the CA distribution mode splitting.

232 The polished plates treated with the R2 medium demonstrated a decrease in the  
 233 hydrophilicity and homogeneity of the surfaces as the StDev had risen and the second  
 234 mode of CA distribution had appeared. At the same time, the first distribution mode

**Table 1** Distribution parameters for wetting contact angle on reference and model surfaces (degrees)

	St.dev.est.*	Minimum of CA observed	Mode 1*	Mode 2*	Maximum of CA observed
	Initial/under R2, 1 month / under R2, 2 months				
Glass	6/4	25/23	43/32	—	54/46
Onyx polishing No 3	3/7/7	28/24/19	32/27/27	—/40/46	38/53/52
Onyx polishing No 4	4	23	32	—	42
Onyx polishing No 2	6	23	32	—	51
Onyx polishing No 1	12	22	35	54	67
Onyx zero polishing	15	33	56	102	120
Gypsum smooth slice	7/4	27/30	40/45	—/72	57/81

\* estimated by Tikhonov and von Mises

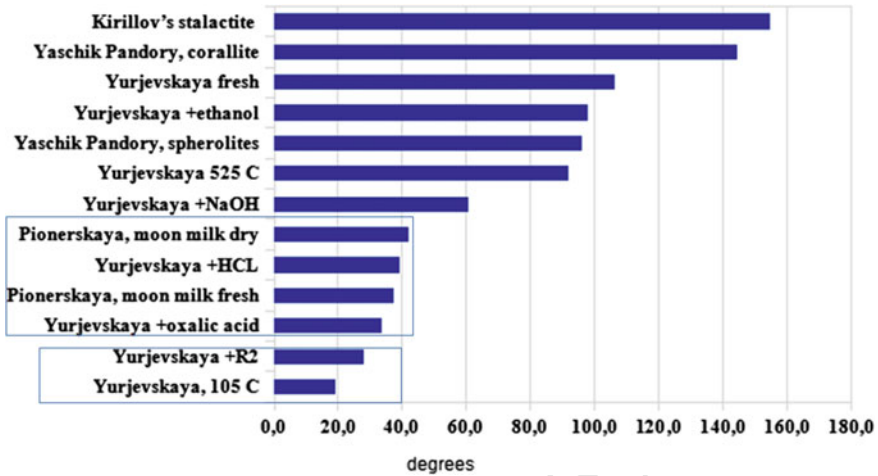


Fig. 2 Euclidean distance between the reference cluster and the samples calculated for wetting contact angle characteristics (min., max., mode 1, mode 2, St.dev.)

and the minimum CA observed shifted toward a more hydrophilic range. This observation is also valid for a gypsum crystal surface. On the contrary, the surface heterogeneity of the calcite speleothem powders under the R2 medium declined, which was indicated by a decrease in the StDev and the disappearance of the hydrophobic CA distribution mode. A similar trend was demonstrated for the silicate glass plate in the homogeneity of the CA distribution and the hydrophilicity of the surface risen under the R2-stimulated biofilm.

CA data was ranged compared to a reference class consisting of flat smooth surface specimens: onyx plates of the *polishing No. 2, 3, 4* and a glass plate treated with the R2 medium (Fig. 2). The reference class showed CA fluctuations in the range of 24° to 44° around an average direction of 32° (by Tikhonov and von Mises) with a StDev estimated as a class average of 4°.

Next, cluster analysis was performed using the K-means algorithm for the independent parameters of the empirical CA distribution as a factor space. This resulted in the CA dataset being combined into 3 subgroups with several members and 4 single values. The first combined subgroup included marble onyx plates after treatment with R2 medium, *polishing No. 1*, specimens of Yuryevskaya Cave dehydrated at 105 °C, treated with oxalic and hydrochloric acids, R2 medium, as well as fresh and dry moon milk from Pionerskaya Cave (Fig. 1c and b). The common features of this subgroup included the unimodal CA distribution, the mode of which was higher than in the reference group, hydrophilicity, and roughness. The surface of the specimens from Yuryevskaya Cave treated with NaOH was distinguished by the transition through the threshold of hydrophobicity. The next subgroup included the specimens from Yuryevskaya Cave treated with ethanol and burning at 525 °C, as well as spherulite formations from the entrance grotto of Yaschik Pandory Cave. That subgroup was characterized by an average CA direction of 58° and CA maximum

261 lying in the hydrophobic area. The last combined subgroup included an untreated  
 262 powder specimen from Yuryevskaya Cave and a *zero polishing* slice of marble onyx.  
 263 There was the CA distribution split into two modes, a hydrophilic one about  $45^\circ$   
 264 and a hydrophobic one about  $100^\circ$  in this group. The differences between the rest  
 265 powder specimens belonging to Yaschik Pandory Cave (corallites with helictites,  
 266 Fig. 1f) and Kirillov's Cave (stalactite) did not allow them to be combined into any  
 267 group, however, all of them were characterized by the low-angle CA mode lied in  
 268 the hydrophilic area whereas the high-angle CA mode had a superhydrophobic range  
 269 and individual CA reached  $140^\circ$ – $150^\circ$ .

270 **SEM, EDX, XRD and DTG analyses.** In most cases, the images show a film gained  
 271 with frequent biomorphs and carbon compared to calcite alone (Fig. 3). On crusts  
 272 filling cracks this film had some differences between the inner smoothed surface  
 273 adjacent to the host rock (dolomite) and the outer subaerial surface regarding the  
 274 ratio of elements (Table 2). There was less carbon on the inner side.

275 When the crusts developed on the bat bones (Fig. 4a) they had the same C/Ca ratio  
 276 as the outer surface of the crack filler, but a higher Ca/O ratio. A peculiar tubular  
 277 structure constituted with crystals elongated along one axis allows us to assume  
 278 confidently aragonite pseudomorphs formed on the initial bone substances. Such an  
 279 aragonite structure may include the “rose” grown on the gypsum surface (Fig. 4b)  
 280 structures of micro-rods with notches of moon milk (Fig. 4d), and helictite needles  
 281 in corallites (Fig. 4c).

282 Figure 5d shows two synchronously recorded thermal analysis curves, namely,  
 283 TG—thermogravimetric curve and DSC—differential scanning calorimetry curve.  
 284 The first indicates the mass loss of the moon milk sample, and the latter shows  
 285 the thermal effects that appear during its burning. The most noticeable changes in

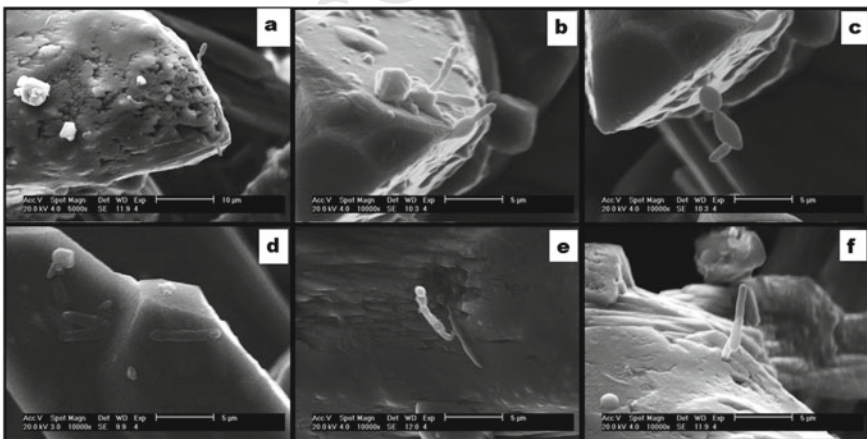


**Fig. 3** Biomorphs on calcite speleothems, Yuryevskaya cave: **a**—a continuous biofilm with prominent biomorphs; **b, c, e, f**—cells penetrated the biofilm surface; **d**—monads on the speleothem surface

**Table 2** Relative content of elements on the surfaces of speleothems and host rocks

Element, %wt	Speleothem crusts				Other speleothems			Gypsum			Dolomite	
	Inner	Extern	Bat bone	+ R2	Lateral	Apex	Apex	“rose”	Initial	+ R2	Initial	+ R2
C	16	18	22	20	12	12	18	—	—	45	13	18
O	42	50	39	53	38	54	58	60	64	41	48	50
Mg	0,4	0,5	0,3	6,0			0,2			0,5	8,9	0,2
Al	0,3	0,6	0,7	0,8	0,7	0,3		0,3	0,2	0,8	1,1	0,2
Si	0,4	0,5	0,3	1,2	0,5	0,3	0,2	0,4	0,1	0,7	5,3	0,3
P				0,3	0,7	0,5	0,4			4,1		1,5
S	0,7	0,4	0,4	0,3				0,9	16,0	0,9	0,3	0,3
K				0,3						0,8	0,4	
Ca	41	30	37	17	47	32	23	38	19	5	21	30
Mn								0,4			0,2	
Fe		0,3		0,3	0,4	0,3	0,4	0,6	0,5		0,6	
C/Ca	0,4	0,6	0,6	1,2	0,3	0,4	0,8	—	—	9,2	0,6	0,6
Ca/O	1,0	0,6	0,9	0,3	1,2	0,6	0,4	0,6	0,3	0,1	0,4	0,6
Ca/P	—	—	—	54,6	65,4	63,1	58,9	—	—	1,2	—	20,7

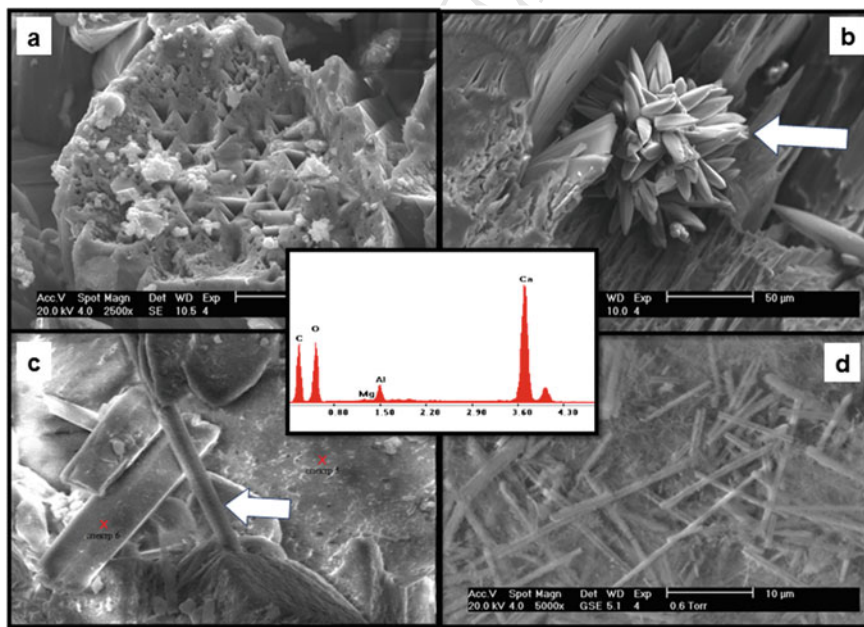
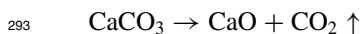


**Fig. 4** Pseudomorphs after aragonite: **a** bat bone from Yurjevskaya cave; **b** “rose” form on gypsum surface from Yurjevskaya cave; **c** micro-rod in corallite from Yaschik Pandory cave; **d** micro-rods in moon milk from Pionerskaya cave

286 the sample are noted in a burning temperature range of 180–500 °C. In this range,  
287 there two exo-effects caused by the thermal dissociation of organic matter are high-  
288 lighted. These two exo-effects manifested at low temperatures and higher tempera-  
289 tures correspond to the dissociation of low and high molecular weight organic matter,  
290 respectively. The total weight loss in this temperature range is 3.5%. The next clear  
291 endo-effect is observed at a temperature of 680–780 °C. Its presence is due to the  
292 thermal dissociation of calcite according to the reaction.



294 Then, one can suppose the formation of calcite pseudomorphs after aragonite  
295 according to XRD and TG-DSC data, since there is present the calcite predomi-  
296 nant phase (91–98%) with the admixture of dolomite, celestite, and quartz in these  
297 tubes (Fig. 5).

298 Based on the results of EDX analysis, the lateral part of the tubular crystals  
299 reproducibly differed in elemental composition from the apical part and approached  
300 organic compounds (Table 2). The presence of phosphorus, which is not common  
301 for the speleothems, also indicates organic inclusions in the crystals.

302 The treatment of calcite speleothems with the R2 medium caused the fixation  
303 of Mg, P, and K elements on the surfaces and a threefold increase in the C/Ca  
304 ratio (Table 2). The appearance of new threads and films over caverns was visually  
305 observed (Fig. 6b, c). The gypsum surface after such treatment was strongly colo-  
306 nized by hyphae-forming microorganisms (Fig. 6f). Herewith high C/Ca ratio, and  
307 precipitation of a new phase containing Mg, P, and K clearly increasing the surface  
308 roughness were observed (Fig. 6d, g, h). The latter is consistent with the previous  
309 investigations that found the phosphate groups released by biofilms to improve their  
310 adhesion to the solid (Andryukov et al. 2020). On the of dolomite surface, the R2  
311 environment caused the appearance of a calcite crust (Table 2).

## 312 4.1 Taxonomic Diversity

313 The clone libraries belonged to 6 major phyla that comprised 10 and 17 OTUs in the  
314 initial speleothems and in the treated with R2 media one, respectively. Proteobacteria  
315 dominated all clone libraries, ranging from 57 to 81% of the clones depending on  
316 the option. About one sixth of the OTUs comprised clones from both options. Phyla  
317 Actinobacteriota and Nitrospirota being quite abundant in the initial speleothems  
318 were suppressed by the R2 medium. Stimulation with the R2 medium was manifested  
319 in the phyla Bacteroidota, Firmicutes, Bdellovibrionota (Table 3).

320 Genera Kribella, Gaiella, and Brevundimonas found in the initial speleothems can  
321 be assigned to the typical extremophiles, and genera Pseudoarthrobacter and Nitro-  
322 spira are obligate chemolithotrophs. R2 media stimulated the most genus Brevundi-  
323 monas, whose representatives are aerobic consumers of organic matter, inhabit  
324 aquatic environments, and have a wide range of resistance to desiccation.

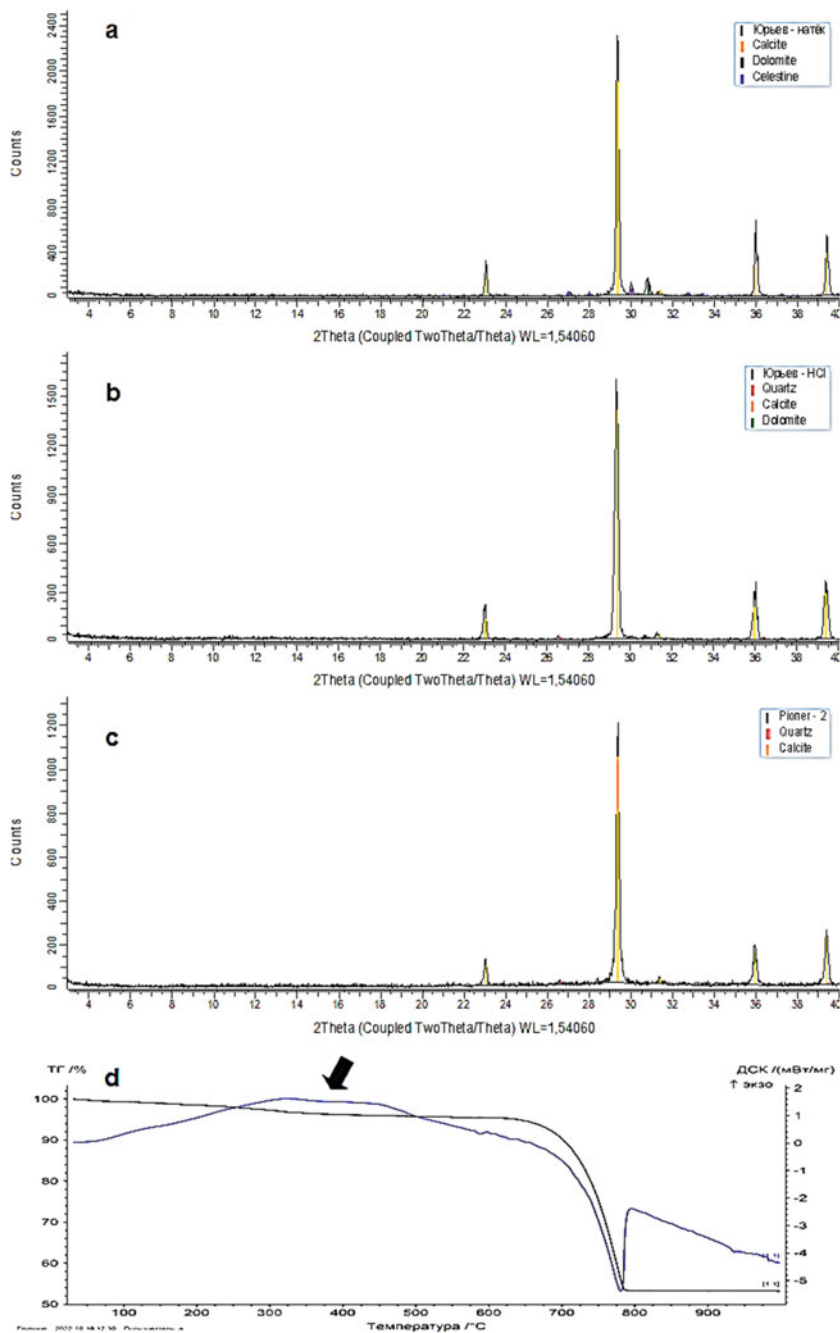


**Fig. 5** The analyses of speleothems: **a** XRD of crusts from Yurjevskaya cave; **b** XRD of crusts etched with HCl from Yurjevskaya cave; **c** XRD of moon milk from Pionerskaya cave; **d** DTG and DSC of moon milk from Pionerskaya cave

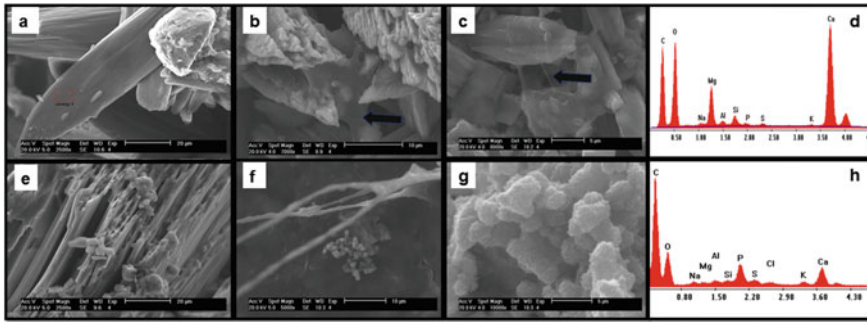


**Fig. 6** The surfaces of calcite crusts (a-d) and gypsum (e-h) from Yurjevskaya Cave before (a and e) and after the stimulation of biofilm with R2 media: b films; c threads; d EDX analysis of the crusts after the stimulation; f hyphae on gypsum slice after the stimulation; g precipitants on gypsum slice after the stimulation; h EDX analysis of gypsum slice after the stimulation

**Table 3** The abundance of bacterial phylla in the crusts of Yurjevskaya cave, %

Option	Initial	+ R2 modified
Proteobacteria	57–77	65–81
Actinobacteriota	16–29	1–1
Nitrospirota	0–4	0
Bacteroidota	0	4–5
Firmicutes	0	2–3
Bdellovibrionota	0	6–7
Total sequence identity	92	96

## 5 Discussion

The CA distributions demonstrate that the speleothem intact surfaces are covered with a partly hydrophobic film. This film was spread as hydrophobic spots with a size of at least 25  $\mu\text{m}$ . Based on infrequent clear individual biomorphs and a high C/Ca ratio, we can confidently attribute the main part of the film to the EPS.

The ratio of the biofilm elements is approximately the same both on the untreated speleothems and speleothems treated with the R2 medium. The difference is manifested only as more clearly defined threads and films covered cavities in crystal surfaces in the latter case (Fig. 6). Samples of both fresh and hardened moon milk were exceptions not forming hydrophobic spots, but they included more than 3% organic matter in their mass too (Fig. 5). Simultaneously, the experiment showed that the development of a biofilm along with hydrophobization can hydrophilize and smooth the surface, i.e. our observations do not contradict each other.

Based on the comparison of surface microanalysis data, one can see that carbon compounds exceed the classical content for calcium carbonate alone, phosphates sometimes appear, and manganese is almost absent, which in total is characteristic



341 of biogenic deposits. The proportions of elements are closest to calcium oxalate in  
342 all samples, but sometimes one can assume the presence of other organic compounds  
343 (malates, succinates, etc.).

344 According to the data presented, the following path of organic matter into the  
345 crystalline matrix can be assumed. Biofilms inhabit fresh carbonate formations  
346 (along the bone, cave milk, feeding channels of corallites and helictites), which  
347 are initially represented by tubular structures of aragonite. Somewhat part of their  
348 EPS gets inside the tubes (but not cells because of the tube diameter of fewer  
349 than 2 microns), and at the same time, the solution is supersaturated with ions in  
350 the tubes (due to selective sorption), which causes precipitation and filling of the  
351 inner cavities. Mixing of the organic and crystallizing phases increases the defec-  
352 tiveness of the crystal lattices formed and declines their energy; thus, aragonite is  
353 replaced by biochemogenic calcite. This process also occurs without the participa-  
354 tion of organic matter (Myszka et al. 2019), but the aragonite structure preservation  
355 observed indicates its acceleration under the biofilm.

356 The roughness could partially reduce the wettability and cause the appearance  
357 of a fuzzy bimodality of the CA distribution, but in no case caused the transition  
358 of the surface properties through the hydrophobicity threshold by itself. Highly  
359 likely, the increase in geometric heterogeneity induced the appearance of preferential  
360 inclination angles of the landing sites for air bubbles.

361 A clear bimodal CA distribution occurs when phases with different surface proper-  
362 ties form clusters and spots, due to which there are both hydrophobic and hydrophilic  
363 areas on the surface, but few areas with intermediate CA values. We observed that  
364 the bimodal distribution of CA appeared only in the following situations: either  
365 the samples were not subjected to any processing other than dispersion or the  
366 treated surface was repopulated with biofilm. Hereby, when fresh biomass devel-  
367 oped, smooth wavy mineral surfaces (calcite and gypsum) able to easily release  
368 cations demonstrated an increase in roughness due to the precipitation of a new  
369 mineral phase and the formation of hyphae, as well as the appearance of hydropho-  
370 bized spots. When cations were difficult to release (e.g., glass), the surface could be  
371 smoothed (healed) by a biofilm.

372 More or less, the hydrophobicity of the speleothem specimens was preserved  
373 after the treatment, decreasing in the set: ethanol, burning, and alkali. However, at  
374 the same time, their bimodality disappeared, i.e., spots of hydrophobic substances  
375 spread over the surface. Other modes of treatment formed the following sequence  
376 with increasing hydrophilicity: hydrochloric acid, oxalic acid, R2 medium, drying at  
377 a temperature of 105 °C, and polishing. Thus, the organic matter extracted from  
378 the mineral matrix partially remains as a film sorbed on the upper layer. This residual  
379 film can be removed due to the etching of minerals, evaporation, and scraping.

380 Genus *Kribella*, *Gaiella*, and *Brevundimonas* found in the original speleothems are  
381 typical extremophiles, while genera *Pseudoarthrobacter* and *Nitrospira* are obligate  
382 chemolithotrophs. The latter genera has the potential for the variable consumption of  
383 organic matter and/or CO<sub>2</sub>, as well as participation in a nitrogen cycle. The modified  
384 R2 media contained organic compounds, therefore it stimulated chemoorganotrophic  
385 growth (e.g., *Brevundimonas*) that suppressed other members of the cave community,

386 which most likely have a low chance of adapting to near-surface soil. In this study,  
387 just like in the metagenomes studied earlier, many microbial types were partly able  
388 to diverge in metabolic pathways, but most of them were heterotrophic (Turrini  
389 et al. 2020). The biofilm autotrophic basis could be the genera *Nitrospira* possessed  
390 the potential for variable consumption of organic matter and/or CO<sub>2</sub>, as well as  
391 participation in a nitrogen cycle. However, the abundance of this genera is not high,  
392 therefore, its ability to provide nutrients for the heterotrophic biomass in a cave  
393 environment is doubtful. In the stimulated community, the functions of the genera  
394 *Nitrospira* as a nitrifier in an environment depleted in organic matter (Daims et al.  
395 2015) were probably transferred to *Pseudomonas* as a heterotrophic nitrifier (Trung  
396 et al. 2019).

397 The hyphae-forming members of phylum Actinobacteria are most likely respon-  
398 sible for an increase in surface roughness. The appearance of hydrophobic groups is  
399 probably the result of the total biofilm secretions, since both their synthesis during the  
400 metabolism of the chemolithoautotrophs and the reverse process of hydrophilization  
401 caused by microbial lytics are possible.

## 402 6 Conclusion

403 The biological changes in minerals depended on metabolic precipitants that either  
404 smoothed or scratched their surfaces. All the fresh speleothems showed higher carbon  
405 in EDX than expected for carbonate alone. Simultaneously, the surface hydropho-  
406 bicity was detected for these samples in a solid state only, which indicated the  
407 hydrophobization of speleothems under long-life biofilms. The spots of a low wetta-  
408 bility were removed from the surfaces by the thermal treatment and washing with  
409 solvents, whereas acid etching and burning of minerals induced the appearance of  
410 such spots. These facts are interpreted as the organic matter is distributed as both  
411 spread on the surface and enclosed in mineral channels. The consumption of the  
412 enclosed organic carbon compounds by biofilms is possible, since we have reason  
413 to believe that the observed cave biofilm community is mostly heterotrophic, with  
414 *Nitrospira* being the only obligate autotrophic among other autochthonous organ-  
415 isms. Nevertheless, there is a lack of organic matter for a heterotrophic nutrition in  
416 all the samples, except fresh moon milk. We can conclude that heterotrophs consume  
417 the organic matter, which can be released and detected only after the destruction of  
418 the crystalline matrix.

419 Then, the storage of nutrients during the periods of their excess, their uptake  
420 and preservation during the crystallization, and the consumption after the mineral  
421 destruction by metabolites can be hypothesized. Such a cycle is possible not only  
422 in caves, but also in subsoils, as well as technogeneuous carbonates. If this dynamic  
423 is confirmed, the surface properties of alike formations should be considered as the  
424 function of organic matter releasing and preserving cycles. The collection of more  
425 complete evidence for this hypothesis requires further research.

426 **Acknowledgements** This paper has been supported by the Kazan Federal University Strategic  
427 Academic Leadership Program (PRIORITY-2030).

428 **Funding** This study was funded by Russian Foundation for Basic Research, project number 20–  
429 05-00,151.

## 430 References

- 431 Andryukov BG, Romashko RV, Efimov TA, Lyapun IN, Bynina MP, Matosova EV (2020) Mecha-  
432 nisms of adhesive-cohesive interaction of bacteria in the formation of a biofilm. *Molekul-*  
433 *yarnaya Genetika, Mikrobiologiya i Virusologiya (Molecular Genetics, Microbiology and*  
434 *Virology)* 35(4):195–201 (in Russian) <https://doi.org/10.17116/molgen202038041155>
- 435 Banks ED, Taylor NM, Gulley J, Lubbers BR, Giarrizo JG, Bullen HA, Hoehler TM and Barton HA  
436 (2010) Bacterial calcium carbonate precipitation in cave environments: a function of calcium  
437 homeostasis. *Geomicrobiology Journal* 27(5):444 — 454. <https://doi.org/10.1080/01490450903485136>
- 438  
439 Callahan BJ, McMurdie PJ, Rosen MJ, Han AW, Johnson AJ, Holmes SP (2016) DADA2: High-  
440 resolution sample inference from Illumina amplicon data. *Nat Methods* 13(7):581–583. <https://doi.org/10.1038/nmeth.3869>
- 441  
442 Daims H, Lebedeva EV, Pjevac P, Han P, Herbold C, Albertsen M, Jehmlich N, Palatinszky M,  
443 Vierheilig J, Bulaev A, Kirkegaard RH, von Bergen M, Rattei T, Bendinger B, Nielsen PH,  
444 Wagner M (2015) Complete nitrification by *Nitrospira* bacteria. *Nature*. 24;528(7583):504–9.  
445 <https://doi.org/10.1038/nature16461>
- 446 D’Angeli IM, Serrazanetti DI, Montanari C, Vannini L, Gardini F, De Waele J (2017) Geochemistry  
447 and microbial diversity of cave waters in the gypsum karst aquifers of Emilia Romagna region,  
448 Italy. *Science of the Total Environment* 598:538–552. <https://doi.org/10.1016/j.scitotenv.2017.03.270>
- 449  
450 Glazovskaya M A and Dobrovolskaya N G (1984) Geochemical functions of microorganisms.  
451 Moscow State University, Moscow (in Russian)
- 452 Golovanova OA (2022) Crystallogenesis in the human body. Dostoevsky Omsk State University,  
453 Omsk (in Russian)
- 454 Gray CJ and Engel AS (2013) Microbial impact on aquifer carbonate geochemistry *The ISME*  
455 *Journal. International Society for Microbial Ecology* 7:325–337. <https://doi.org/10.1038/ismej.2012.105>
- 456  
457 Guvensen NC, Demir S, Ozdemir G (2013) Effects of magnesium and calcium cations on biofilm  
458 formation by *Sphingomonas paucimobilis* from an industrial environment. *Current Opinion in*  
459 *Biotechnology* 24(1):S68. <https://doi.org/10.1016/j.copbio.2013.05.185>
- 460 Klindworth A, Pruesse E, Schweer T, Peplies J, Quast C, Horn M, Glöckner FO (2013) Evaluation  
461 of general 16S ribosomal RNA gene PCR primers for classical and next-generation sequencing-  
462 based diversity studies. *Nucleic acids research* 41(1): e1. <https://doi.org/10.1093/nar/gks808>
- 463 Leonova LV, Kuz’mina LY, Ryabova AS, Simakova YS, Glavatskikh SP, Cherviatcova OY (2015)  
464 Modern nodules: mineralogical investigation and modelling experiments. *Vestnik IG Komi SC*  
465 *UB RAS* 10:45–51 <https://doi.org/10.19110/2221-1381-2015-10-45-51>
- 466 McMurdie PJ, Holmes S (2013) Phyloseq: An R package for reproducible interactive analysis and  
467 graphics of microbiome census data. *PLoS ONE* 8(4):e61217. <https://doi.org/10.1371/journal.pone.0061217>
- 468  
469 Melim LA, Northup DE, Boston PJ, Spilde MN (2016) Preservation of fossil microbes and biofilm  
470 in cave pool carbonates and comparison to other microbial carbonate environments. *PALAIOS*  
471 31:177–189. <https://doi.org/10.2110/palo.2015.033>

- 472 Mouraviev FA, Vinokurov VM, Galeev AA et al. (2006) Paramagnetism and the nature of dispersed  
473 organic matter in the Permian deposits of Tatarstan. *Georesources* 2(19):40-45 (in Russian)
- 474 Myszka B, Schußler M, Hurlle K, Demmert B, Detsch R, Boccaccini AR, Wolf SE (2019) Phase-  
475 specific bioactivity and altered Ostwald ripening pathways of calcium carbonate polymorphs in  
476 simulated body fluid. *Royal Soc of Chem Adv.* 9:18232–18244
- 477 Nomokonov VE (1969) On the stratigraphy of the Upper Cambrian and Cambrian deposits in the  
478 region of Yefremkino and Malaya Syja settlements. *Izvestiya Tomskogo politeknicheskogo*  
479 *instituta* 196:40-47 (in Russian)
- 480 Pronk GJ, Heister K, Vogel C et al. (2017) Interaction of minerals, organic matter, and microor-  
481 ganisms during biogeochemical interface formation as shown by a series of artificial soil  
482 experiments. *Biology and Fertility of Soils* 53:9–22. <https://doi.org/10.1007/s00374-016-1161-1>
- 483 Sofinskaya OA, Kosterin AV, Galeev AA (2022) Heterogeneity of Wetting Contact Angle in  
484 Hydrophobized Soils and Parent Rocks. *Eurasian Soil Sc.* 55:339–347. <https://doi.org/10.1134/S1064229322030139>
- 485
- 486 Trung TT, Bott NJ, Dai Lam N, Trung NN, Hoang Thi Dang O, Hoang Le D, Tung Le L, Hoang  
487 Chu H (2019) The role of pseudomonas in heterotrophic nitrification: a case study on shrimp  
488 ponds (*Litopenaeus vannamei*) in soc trang province. *Microorganisms.* 29:7(6):155. <https://doi.org/10.3390/microorganisms7060155>
- 489
- 490 Tugarova MA (2021) Indicator signs of carbonate microbialites in black shale formations: isotopic  
491 composition and biomarkers. *Vestnik of geosciences* 11(323):55-61. <https://doi.org/10.19110/geov.2021.11.5>
- 492
- 493 Turrini P, Tescari M, Visaggio D, Pirolo M, Lugli GA, Ventura M, Frangipani E, Visca P (2020)  
494 The microbial community of a biofilm lining the wall of a pristine cave in Western New Guinea  
495 *Microbiological Research* 241:126584
- 496 Wagner M and Horn H (2017) Optical coherence tomography in biofilm research: A comprehen-  
497 sive review. *Biotechnology and Bioengineering* 114(7):1386-1402. <https://doi.org/10.1002/bit.26283>
- 498
- 499 Wiseschart A, Mhuantong W, Tangphatsornruang S, Chantasingh D, Pootanakit K (2019) Shotgun  
500 metagenomic sequencing from Manao-Pee cave, Thailand, reveals insight into the microbial  
501 community structure and its metabolic potential. *BMC Microbiol.* 19:144
- 502 Zorina AS, Maksimova YG, Demakov VA (2019) Biofilm formation by monocultures and mixed  
503 cultures of *Alcaligenes Faecalis* 2 and *Rhodococcus Ruber* Gt 1. *Microbiology* 88(2):164-171.  
504 <https://doi.org/10.1134/S0026261719020140>

# Author Queries

## Chapter 29

Query Refs.	Details Required	Author's response
AQ1	<p>Please be aware that your name and affiliation and if applicable those of your co-author(s) will be published as presented in this proof. If you want to make any changes, please correct the details now. Please note that after publication corrections won't be possible. Due to data protection we standardly publish professional email addresses, but not private ones, even if they have been provided in the manuscript and are visible in this proof. If you or your co-author(s) have a different preference regarding the publication of your mail address(s) please indicate this clearly. If no changes are required for your name(s) and affiliation(s) and if you agree with the handling of email addresses, please respond with "Ok".</p>	